Computational Biology and Chemistry 72 (2018) 77–86

Contents lists available at ScienceDirect

Computational Biology and Chemistry

journal homepage: www.elsevier.com/locate/compbiolchem

Research Article

An integrative *in silico* approach to the structure of Omp33-36 in *Acinetobacter baumannii*

Abolfazl Jahangiri[a], Iraj Rasooli[b,*], Parviz Owlia[c,d], Abbas Ali Imani Fooladi[e], Jafar Salimian[f]

[a] Department of Biology, Shahed University, Tehran, Iran
[b] Department of Biology, Shahed University, Tehran-Qom Express Way, Tehran, Iran
[c] Department of Microbiology, Shahed University Faculty of Medical Sciences, Tehran, Iran
[d] Molecular Microbiology Research Center (MMRC), Shahed University, Tehran, Iran
[e] Applied Microbiology Research Center, Baqiyatallah University of Medical Sciences, Tehran, Iran
[f] Chemical Injuries Research Center, Baqiyatallah University of Medical Sciences, Tehran, Iran

ARTICLE INFO

Article history:
Received 31 March 2017
Received in revised form 7 January 2018
Accepted 10 January 2018
Available online 12 January 2018

Keywords:
Omp34
Bioinformatic
A. baumannii
Structure prediction
Topology
Secondary structure

ABSTRACT

Omp33-36 in *A. baumannii*, a bacterium causing serious nosocomial infections, is a virulence factor associated with the pathogen metabolic fitness as well as its adherence and invasion to human epithelial cells. This protein is also involved in interaction of the bacteria with host cells by binding to fibronectin. Moreover, Omp33-36 renders cytotoxicity to *A. baumannii* in addition to inducing apoptosis and modulation of autophagy. In the present study, an integrated strategy is launched to pierce into the 3D structure of Omp33-36 protein. The signal peptide within the sequence was determined, then, topology as well as secondary and tertiary structures of the protein were predicted. The mature protein assigned as a 14-stranded barrel in which residues 1–19 is removed as signal peptide. The obtained 3D models were evaluated in terms of quality; and then, served as queries to find similar protein structures. The hits were analyzed regarding topology among which 14-stranded were considered. The most qualified model was refined and then its sequence aligned to its counterpart similar structure protein (CymA from *Klebsiella oxytoca*). The determined structure of Omp33-36 could justify its porin function and carbapenem-resistance associated with the loss of this protein.

1. Introduction

Acinetobacter baumannii, a Gram-negative, non-motile coccobacillus (Martí et al., 2006), causes serious nosocomial infections including pneumonia, meningitis, urinary tract infections, skin and soft tissue infections and bloodstream infections (McConnell et al., 2013). Owing to the emergence of highly antibiotic-resistant strains including multidrug-resistant and pan-drug resistant, conquering to these infections become more difficult (Dijkshoorn et al., 2007; Wang et al., 2003). Mortality rate of *A. baumannii*-associated infections could be up to 70% (Vila and Pachón, 2012). In spite of its high mortality, a few potential virulence factors have been investigated (McConnell et al., 2013; Smani et al., 2013). Recently, Omp33-36 has been ascribed as a virulence factor associated with metabolic fitness of *A. baumannii* as well as the pathogen adherence and invasion to human epithelial cells. This protein could bind to fibronectin and thereby play a substantial role in interaction of *A. baumannii* to host cells (Smani et al., 2012). Moreover, this essential virulence factor for infection in animal models is one of several proteins rendering cytotoxicity to *A. baumannii* (Smani et al., 2013). In human cells, Omp33-36 could induce apoptosis and modulate autophagy (Rumbo et al., 2014). This protein enables the pathogen to persist inside autophagosomes *via* inhibition of autophagy (Rumbo et al., 2014). A mutant Omp33-36 strain has exhibited higher lethal dose and lesser dissemination in a murine sepsis model (Smani et al., 2013). In addition to its important roles in virulence of *A. baumannii*, the protein is nominated as a strong immunogen by various researchers (Fajardo Bonin et al., 2014; Islam et al., 2011; McConnell et al., 2011). McConnell et al. used outer membrane vesicles (OMVs) released in extracellular space by *A. baumannii*

* Corresponding author at: Department of Biology, Shahed University, Tehran-Qom Express Way, Opposite Imam Khomeini's shrine, Tehran-3319118651, Iran.
E-mail address: rasooli@shahed.ac.ir (I. Rasooli).

https://doi.org/10.1016/j.compbiolchem.2018.01.003
1476-9271/

ATCC 17978 as a vaccine candidate against the pathogen and shown that the outer membrane protein is enriched in the OMVs (McConnell et al., 2011). Islam et al. demonstrated that the protein could serve as a specific antigen for detection of *A. baumannii* (Islam et al., 2011). Recently, an immunoproteomic study on the pathogen revealed that this protein is an appropriate vaccine candidate against *A. baumannii* (Fajardo Bonin et al., 2014).

Despite of its remarkable functions and immunological properties, no comprehensive attempt is carried out to unveil Omp33-36 three-dimensional structure. Tertiary structure of proteins paving the way for insight into the protein functions as well as its interactions with other molecules (Mihăşan, 2010). Moreover, conformational epitope predictions and vaccine design could benefit from a high resolution unveiled structure (Haste Andersen et al., 2006; Khalili et al., 2014; Nezafat et al., 2016; Sefid et al., 2015). In addition to facing high failure rate, experimental determination of 3D protein structures is time consuming and expensive (Petrey and Honig, 2005). Obstacles are more highlighted in the case of outer membrane proteins due to difficulty in their purification as a functional transmembrane protein (Lacapere et al., 2007). Several researchers have invoked bioinformatic tools as an alternative to conquering snags ahead in experimental determination of protein structures (Gaete-Eastman et al., 2015; Jahangiri et al., 2017; Khalili et al., 2016; Khalili et al., 2017a; Khalili et al., 2017b; Malathi et al., 2017; Mohammadpour et al., 2015; Mohammadpour et al., 2016; Sefid et al., 2013). Nowadays several up-to-date robust methods and services such as I-TASSER (Yang et al., 2015), RaptorX (Källberg et al., 2012), Phyre2 (Kelley et al., 2015) and ROBETTA (Kim et al., 2004) are developed which could introduce 3D structure of a protein from its sequence. Three approaches are often considered in protein structure predictions: homology or comparative modeling, fold recognition (threading) and *ab initio*. Homology modeling refers to the process of model building from a single template found in the PDB with high sequence similarity to the target protein. Fold recognition would be employed where similar templates to the target, existing in the PDB, could not easily be identified. *ab initio* recruit physics and chemistry rules to predict protein structure where no similar template is found in the PDB (reviewed in (Petrey and Honig, 2005)).

In the current study, various *in silico* approaches are employed to unveil and validate the 3D structure of Omp33-36 protein.

2. Methods

2.1. Sequence availability

In order to performing bioinformatic analyses, the reference sequence of Omp34 kDa protein with accession no. WP_000733005.1 obtained from NCBI at http://www.ncbi.nlm.nih.gov/protein was saved in FASTA format.

2.2. Sequence-based protein classification

BOMP (Berven et al., 2004) at http://services.cbu.uib.no/tools/bomp/ was employed to ascertain whether the sequence is an integral β-barrel outer membrane protein. This server ranks integral outer membrane proteins from 1 to 5 where 1 is the least reliable prediction, and 5 is the most reliable (Berven et al., 2004). To enhance prediction reliability, MCMBB (Bagos et al., 2004a) at http://athina.biol.uoa.gr/bioinformatics/mcmbb/, HHomp (Remmert et al., 2009) at http://toolkit.tuebingen.mpg.de/hhomp and TMBETADISC-RBF (Ou et al., 2008) at http://rbf.bioinfo.tw/~sachen/OMPpredict/TMBETADISC-RBF.php were also used. MCMBB discriminates beta-barrel outer membrane proteins from globular proteins and alpha-helical membrane proteins with accuracy of >90%. A protein sequence scored greater than zero is assigned as a beta-barrel outer membrane protein (Bagos et al., 2004a). HHomp is a method for protein homology detection and classification of OMP. It builds a profile hidden Markov model (HMM) from a query sequence and compares it with a database of HMMs representing outer membrane proteins by invoking an integrated beta-barrel prediction method (Remmert et al., 2009). TMBETADISC-RBF is a method (accuracy >95%) based on radial basis function networks and position specific scoring matrix (PSSM) profiles (Ou et al., 2008). Efflux-RBF (Ou et al., 2013) at http://rbf.bioinfo.tw/~sachen/EFFLUXpredict/Efflux-RBF.php was harnessed to predict whether the protein is belonging to efflux proteins. Efflux-RBF prediction is based on radial basis function networks invoking amino acid properties and position specific scoring matrices (PSSM) with prediction accuracy of ≥78 (Ou et al., 2013). Transporter-RBF (Ou et al., 2010) at http://rbf.bioinfo.tw/~sachen/TCpredict/Transporter-RBF.php was employed to predict protein classification. Transporter-RBF is a radial basis function (RBF) network method based on position specific scoring matrix profiles discriminating transporters with accuracy of ≥69% (Ou et al., 2010).

2.3. Crystallization analyses

The protein crystallizability was predicted by XtalPred (Slabinski et al., 2007) at http://ffas.burnham.org/XtalPred-cgi/xtal.pl. This server estimates crystallization possibility of the submitted protein by comparing its predicted biochemical and biophysical properties with those calculated from TargetDB. XtalPred uses two methods for crystallization classifications: Expert Pool and Random Forest; In the Expert Pool method, individual crystallization probabilities calculated for eight protein features (length, isoelectric point, gravy index, predicted structural disorder, instability index, predicted coil secondary structure, predicted coiled-coil structure and insertion score) are combined into a single crystallization score. Based on the obtained score, the query protein will be assigned as one of five crystallization classes (optimal, suboptimal, average, difficult and very difficult) (Slabinski et al., 2007). Random Forest classifier uses an extended list of protein features in which hydrophobicity, amino-acid composition of the predicted protein surface, predicted surface ruggedness and side-chain entropy of surface residues are added (Jahandideh et al., 2014).

2.4. Signal peptide and topology prediction

The protein sequence served as an input data for SignalP 4.1 (Bagos et al., 2004b) at http://www.cbs.dtu.dk/services/SignalP-4.1/ to predict probable signal peptide within the sequence. Moreover, LipoP 1.0 (Juncker et al., 2003) at http://www.cbs.dtu.dk/services/LipoP/ was employed to assign signal peptidase I or II cleavage sites within the protein. In order to pierce into potential transmembrane β-strands, the protein sequence was fed as an input to 2 different servers: PRED-TMBB (Bagos et al., 2004b) at http://bioinformatics.biol.uoa.gr/PRED-TMBB/and BOCTOPUS (Hayat and Elofsson, 2012) at http://boctopus.cbr.su.se/index.php. The analyses were performed on the full-length and the mature (without signal peptide) protein sequences. PRED-TMBB is a Hidden Markov Model method discriminating beta-barrel outer membrane proteins and predicting their transmembrane beta-strands (Bagos et al., 2004b). BOCTOPUS uses separate SVMs and a Hidden markov model (HMM) to predict topology (the number of beta strands and in and out loop location) of putative transmembrane beta barrel proteins (Hayat and Elofsson, 2012).

2.5. Secondary structure prediction

The protein sequence served as an input to SYMPRED (Simossis and Heringa, 2004) at http://www.ibi.vu.nl/programs/sympredwww/, Jpred4 (Drozdetskiy et al., 2015) at http://www.compbio.dundee.ac.uk/jpred4/index.html and SEGMER (Wu and Zhang, 2010) at http://zhanglab.ccmb.med.umich.edu/SEGMER/ to determine its secondary structure. SYMPRED is a consensus-deriving secondary structure predictor which employs the PSI-BLAST algorithm to produce input for the individual methods used. The consensus result with high accuracy is derived through dynamic programming (Simossis and Heringa, 2004). Jpred4, the latest version of Jpred, uses the JNet algorithm to predict protein secondary structure. This server predict three-state (α-helix, β-strand and coil) secondary structure with accuracy of >80.0% (Drozdetskiy et al., 2015). SEGMER is a segmental threading algorithm could recognize substructure motifs from the Protein Data Bank (PDB) library. This server splits the target sequence into segments consisting of 2–4 consecutive or non-consecutive secondary structure elements (alpha-helix, beta-strand). Then, thread the segments through the PDB to identify conserved substructures (Wu and Zhang, 2010).

2.6. 3D structure prediction

2.6.1. Template search and homology modeling

In order to arrive at an appropriate template, the Omp34 kDa protein sequence served as a query for PSI-BLAST against PDB at http://blast.ncbi.nlm.nih.gov/Blast.cgi. Memoir (Ebejer et al., 2013) at http://opig.stats.ox.ac.uk/webapps/memoir/php/index.php was used for predicting 3D structure of the protein. This server is a homology modeling algorithm designed for membrane proteins (Ebejer et al., 2013). The best hit obtained from PSI-BLAST was used as a template and signal peptide of the input sequence was removed.

2.6.2. Other approaches

In addition to homology modeling, various servers with different approaches were used to build an accurate 3D model: eThread (Brylinski and Lingam, 2012) at http://brylinski.cct.lsu.edu/content/webservices integrates ten state-of-the-arts threading/fold recognition algorithms and employs various machine learning techniques to perform the template-based protein structure modeling. FALCON@home (Wang et al., 2015) at http://protein.ict.ac.cn/TreeThreader/ is a high-throughput protein structure prediction server based on remote homologue identification. This tool first find conserved regions from each template and then aligns a query protein with these regions rather than the full-length template. I-TASSER (Yang et al., 2015) at http://zhanglab.ccmb.med.umich.edu/I-TASSER/ is a hierarchical method for protein structure and function prediction. This tool identifies structural templates from the PDB using multiple threading approach LOMETS. Then, it constructs full-length atomic models by iterative template fragment assembly simulations. LOMETS (Wu and Zhang, 2007) at http://zhanglab.ccmb.med.umich.edu/LOMETS/ is a Local Meta-Threading-Server for protein structure prediction. The 3D models are built by using high-scoring target-to-template alignments from 9 threading programs (FFAS-3D, HHsearch, MUSTER, pGenTHREADER, PPAS, PRC, PROSPECT2, SP3, and SPARKS-X). Phyre2 (Kelley et al., 2015) at http://www.sbg.bio.ic.ac.uk/phyre2/html/page.cgi?id=index uses advanced remote homology detection methods to generate 3D models, predict ligand binding sites and analyze the effect of amino acid variants for a given protein sequence. ROBETTA (Kim et al., 2004) at http://robetta.bakerlab.org/ is a full-chain protein structure predictor parsing protein chains into putative domains with the Ginzu protocol, and models the obtained domains by homology or *ab initio* modeling. RaptorX (Källberg et al., 2012) at http://raptorx.uchicago.edu/ is a statistical method for template-based protein structure prediction. Alignment accuracy of this tool is improved by exploiting structural information in a single or multiple templates which enable it predicting 3D structures of protein sequences without close homologs in the Protein Data Bank (PDB).

In all 3D model predictions, signal peptide was removed from the query sequence.

2.6.3. Model evaluation and screening

Models covering full-length of the mature protein were evaluated by QMEAN (Benkert et al., 2009) at http://swissmodel.expasy.org/qmean/cgi/index.cgi. QMEAN (Qualitative Model Energy ANalysis) estimates the quality of protein structure models and describes the major geometrical aspects of protein structures. Five different structural descriptors analyzed by the server are including the local geometry, long-range interactions, the burial status of the residues and two simple terms describing the agreement of predicted and calculated secondary structure and solvent accessibility. Moreover, the Ramachandran plot for each model was depicted by RAMPAGE at http://mordred.bioc.cam.ac.uk/~rapper/rampage.php. In addition to estimation of model quality by above servers, the best models were also manually assessed with respect to complying with secondary structure as well as topology of the protein predicted in previous steps. PhyreStorm (Mezulis et al., 2016) at http://www.sbg.bio.ic.ac.uk/~phyrestorm/phyrestorm/index.html was used to rapidly and comprehensively compare predicted protein structures to the entire PDB. TM score cutoff was set as 0.6. Hits were evaluated in regard of possessing potential transmembrane β-strands by PRED-TMBB and BOCTOPUS2.

2.6.4. Model refinement

The best model passed the previous step was fall into model refinement process. Three different servers were invoked for this task: ModRefiner (Xu and Zhang, 2011), 3Drefine (Bhattacharya et al., 2016) and GalaxyRefine (Heo et al., 2013). ModRefiner at http://zhanglab.ccmb.med.umich.edu/ModRefiner/ was harnessed for high-resolution protein structure refinement at atomic-level. The refinement could be started from C-alpha trace, main-chain model or full-atomic model. ModRefiner has an option to allow for the assignment of a second structure which will be used as a reference to which the refinement simulations are driven. This option was also employed in which 4D5B_A served as a template structure. One aim of ModRefiner is to draw the initial starting models closer to their native state, in terms of hydrogen bonds, backbone topology and side-chain positioning. It also generates significant improvement in physical quality of local structures. 3Drefine at http://sysbio.rnet.missouri.edu/3Drefine/index.html could efficiently refine protein structures using iterative optimization of hydrogen bonding network in combination with atomic-level energy minimization on the optimized model by knowledge-based force fields and a composite physics. GalaxyRefine at http://galaxy.seoklab.org/cgi-bin/submit.cgi?type=REFINE first performs side-chain rebuilding and repacking and then, overall structure relaxation by molecular dynamics simulation. Quality of refined models was evaluated by Qmean and RAMPAGE.

2.7. Sequence alignment

The sequence of Omp34 kDa was aligned to the protein sequence of 4D5B_A by PRALINE (Pirovano et al., 2008) at http://www.ibi.vu.nl/programs/pralinewww/

2.8. Data validation

In addition to employing the state-of-the-art servers through all steps of the workflow, two or more tools or methods were invoked for each analysis to enhance the results accuracy. An integrative strategy (combination of sequence-based protein classification, topology, secondary structure, 3D structure,) was employed to achieve a more confident model. Moreover, in order to arriving at the most reliable results, prediction results were combined with previous experimental evidence.

3. Results

3.1. Protein classification

BOMP predicted the protein as an integral β-barrel outer membrane protein with rank as high as 4. MCMBB scored the protein 0.055 as a β-barrel outer membrane protein. Overall probability for the query to be an OMP was determined 100% by HHomp. TMBETADISC-RBF also predicted the query as an outer membrane protein. The protein was not classified as an efflux protein. Transporter-RBF classified the query protein as a β-barrel channel/pore.

3.2. Crystallization probability

Based on Expert Pool method, the protein could be crystallized very difficult (scored as 5). This method classifies protein crystallizations as follow: optimal (1), suboptimal (2), average (3), difficult (4) or very difficult (5). Crystallization classification of the protein was scored as 8 by Random Forest classifier. This classifier could scoring proteins as 1–11 in which 1 refers to the most promising and 11 refers to the least promising crystallization targets.

3.3. Signal peptide and protein topology

Position 1–19 of the protein sequence predicted as signal peptide which its cleavage site (between position 19 and 20) could be cleaved by signal peptidase I. Fourteen transmembrane β-strands were predicted by specialized servers, BOCTOPUS and PRED-TMBB. Distribution of residues in the topology is as following: 122 (40.8%) transmembrane β-strand, 63 (21.07%) cytosolic side and 114 (38.13%) extracellular side; 124 (41.47%) transmembrane β-strand, 46 (15.38%) cytosolic side and 129 (43.14%) extracellular side predicted by BOCTOPUS and PRED-TMBB respectively. Details of topology as a transmembrane beta-barrel protein are depicted in Fig. 1 and Table 1.

3.4. Secondary structure

SYMPRED predicted 123 residues (41.14%) as strand and 29 residues (9.7%) as helix. Jpred4 predicted 134 (44.8%) and 22 (7.3%) residues as these elements of structure respectively. Thirty-six (12%), 126 (42.14%) residues were predicted as helix and strand respectively by SEGMER. Details of Omp34 kDa secondary structure are presented in Fig. 2.

3.5. Three-dimensional structure

The best hit obtained from PSI-BLAST with 10 iterations was a sequence with Acc. no. 3VCY_A (query coverage: 23%, E value: 2e-18 and identity: 14%). Prediction of 3D structure by “Memoir” was failed since no iMembrane hits found for template (3VCY_A)

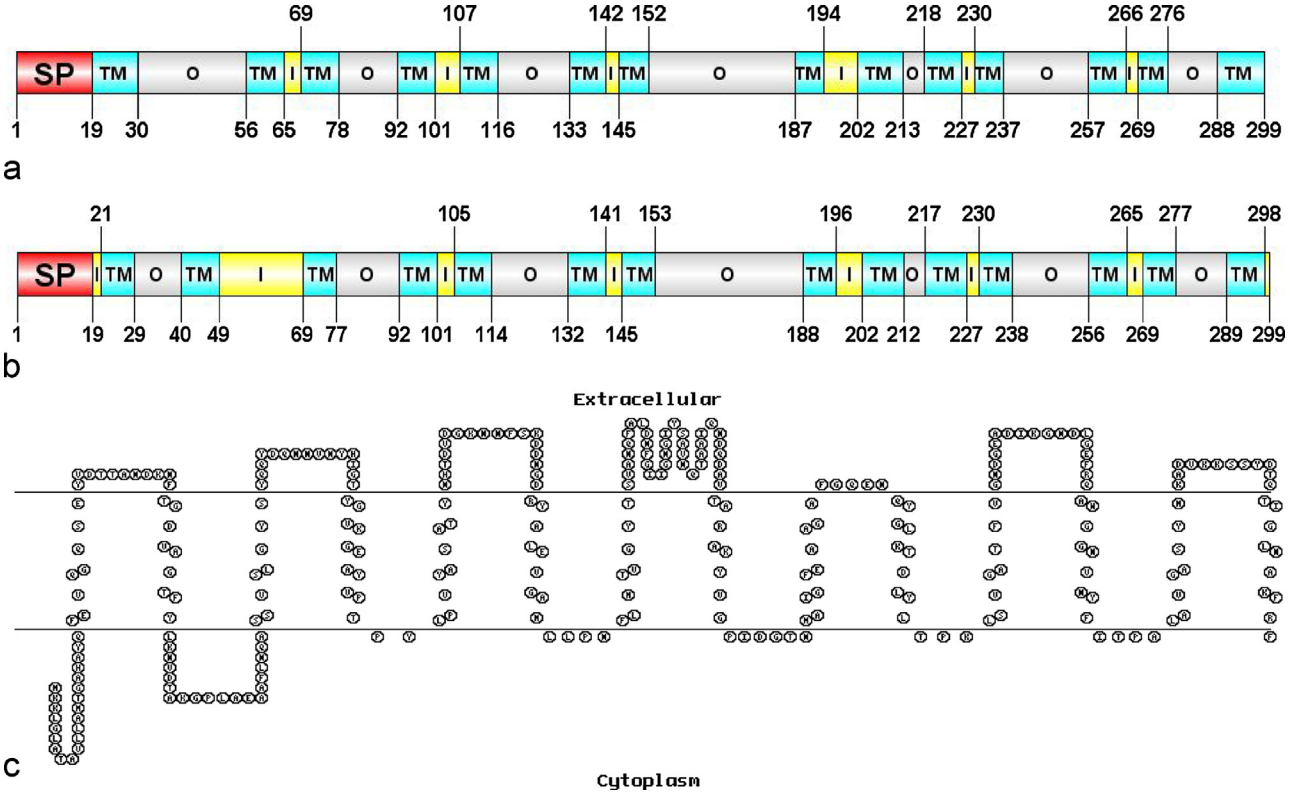

Fig. 1. (a–c) Topology of the Omp34 protein illustrated based on PRED-TMBB (a) and BOCTOPUS (b) predictions. Schematic 2D topology of the Omp34 protein illustrated based on BOCTOPUS prediction (c).

Table 1
Topology components of Omp33-36. Residues and the numbers of them involved in topology components.

PRED-TMBB		BOCTOPUS	
Topology components	Sequence/Residues numbers	Topology components	Sequence/Residues numbers
β1	YQFEVQGQSEY/Y:2, Q:3, F:1, E:2, V:1, G:1,S:1	In1	YQ/Y:1, Q:1
Out1	VDTTANDKNFTGDVAGTFYLK/V:2, D:3, T:4, A:2, N:2, K:2, F:2, G:2, Y:1, L:1	β1	FEVQGQSE/F:1, E:2, V:1, Q:2, G:1, S:1
β2	KGPLAEAAF/K:1, G:1, P:1, L:1, A:3, E:1, F:1	Out1	YVDTTANDKNF/Y:1, V:1, D:2, T:2, A:1, N:2, K:1, F:1
In1	LNQA/L:1, N:1, Q:1,A:1	β2	TGDVAGTFY/T:2, G:2, D:1, V:1, A:1, F:1, Y:1
β3	SSVSLGYSY/S:4, V:1, L:1, G:1, Y:2	In2	LKNVDTAKGPLAEAAFLNQA/L:3, K:2, N:2, V:1, D:1, T:1, A:5, G:1, P:1, E:1, F:1, Q:1
Out2	QQYDQNNVNYHIGT/Q:3, Y:2, D:1, N:3, V:1, H:1, I:1, G:1, T:1	β3	SSVSLGYS/S:4, V:1, L:1, G:1, Y:1
β4	YGVKGEAYV/Y:2, G:2, V:2, K:1,E:1, A:1	Out2	YQQYDQNNVNYHIGT/Y:3, Q:3, D:1, N:3, V:1, H:1, I:1, G:1, T:1
In2	PTPYLP/P:3, T:1, Y:1, L:1	β4	YGVKGEAYV/Y:2, G:2, V:2, K:1, E:1, A:1
β5	VYASATYNH/V:1, Y:2, A:2, S:1, T:1, N:1, H:1	In3	PTPY/P:2, T:1, Y:1
Out3	TDVDGKNNFSKDDNGDR/T:1, D:5, V:1, G:2, K:2, N:3, F:1, S:1, R:1	β5	LPVYASATY/L:1, P:1, V:1, Y:2, A:2, S:1, T:1
β6	YALEVGAML/Y:1, A:2, L:2, E:1, V:1, G:1, M:1	Out3	NHTDVDGKNNFSKDDNGD/N:4, H:1, T:1, D:5, V:1, G:2, K:2, F:1, S:1,
In3	LPN/L:1, P:1, N:1	β6	RYALEVGAM/R:1, Y:1, A:2, L:1, E:1, V:1, G:1, M:1
β7	FLMTVGY/F:1, L:1, M:1, T:1, V:1, G:1, Y:1	In4	LLPN/L:2, P:1, N:1
Out4	TSVANQFALDNFGIIGNGIYSAVNQTAAIQNDQDA/T:2, S:2, V:2, A:6, N:5, Q:4, F:2, L:1, D:3, G:3, I:4, Y:1,	β7	FLMTVGYT/F:1, L:1, M:1, T:2, V:1, G:1, Y:1
β8	VTARAKY/V:1, T:1, A:2, R:1, K:1, Y:1	Out4	SVANQFALDNFGIIGNGIYSAVNQTAAIQNDQDAV/S:2, V:3, A:6, N:5, Q:4, F:2, L:1, D:3, G:3, I:4, Y:1, T:1,
In4	VGPIDGTN/V:1, G:2, P:1, I:1, D:1, T:1, N:1	β8	TARAKYVG/T:1, A:2, R:1, K:1, Y:1, V:1, G:1
β9	MAIGFEAAGAF/M:1, A:4, I:1, G:2, F:2, E:1	In5	PIDGTN/P:1, I:1, D:1, G:1, T:1, N:1
Out5	GQENQ/G:1, Q:2, E:1, N:1	β9	MAIGFEAAGA/M:1, A:4, I:1, G:2, F:1, E:1
β10	YGLKTDLYL/Y:2, G:1, L:3, K:1, T:1, D:1	Out5	FGQEN/F:1, G:1, Q:1, E:1, N:1
In5	TPK/T:1, P:1, K:1	β10	QYGLKTDLYL/Q:1, Y:2, G:1, L:3, K:1, T:1, D:1
β11	LSVGATF/L:1, S:1, V:1, G:1, A:1, T:1, F:1	In6	TPK/T:1, P:1, K:1
Out6	VGNDGEADIKGNDLGEFRQA/V:1, G:4, N:2, D:3, E:2, A:2, I:1, K:1, L:1, F:1, R:1, Q:1	β11	LSVGATFV/L:1, S:1, V:2, G:1, A:1, T:1, F:1
β12	WGGNVNYFI/W:1, G:2, N:2, V:1, Y:1, F:1, I:1	Out6	GNDGEADIKGNDLGEFRQ/G:4, N:2, D:3, E:2, A:1, I:1, K:1, L:1, F:1, R:1, Q:1
In6	TPA/T:1, P:1, A:1	β12	AWGGNVNYF/A:1, W:1, G:2, N:2, V:1, Y:1, F:1
β13	LAVGASY/L:1, A:2, V:1, G:1, S:1, Y:1	In7	ITPA/I:1, T:1, P:1, A:1
Out7	MKADVKKSSYDT/M:1, I:1, K:3, A:1, D:2, V:1, S:2, Y:1, T:1	β13	LAVGASYM/L:1, A:2, V:1, G:1, S:1, Y:1, M:1
β14	QTIGLNAKFRF/Q:1, T:1, I:1, G:1, L:1, N:1, A:1, K:1, F:2, R:1	Out7	KADVKKSSYDTQ/K:3, A:1, D:2, V:1, S:2, Y:1, T:1, Q:1
		β14	TIGLNAKFR/T:1, I:1, G:1, L:1, N:1,A:1, K:1, F:1, R:1
		In8	F/F:1
Total residues of In	L:3, N:3, Q:1, A:2, P:7, T:4, Y:1, V:1, G:1, I:1, D;1	Total residues of In	Y:2, Q:2, T:5, L:5, K:3, N:4, V:1, D:2, A:6, G:2, P:7, E:1, F:2, I:2,
Total residues of β	Y:15, Q:4, F:9, E:6, V:11, G:15, S:8, K:5, P:1, L:11, A:18, T:6, N:4, H:1, M:3, R:2, I:3, D:1, W:1	Total residues of β	F:7, E:5, V:13, Q:3, G:17, S:8, T:9, D:2, A:17, Y:13, L:10, K:4, P:1, R:3, M:3, I:2, W:1, N:3
Total residues of Out	V:8, D:17, T:9, A:11, N:16, K:8, F:6, G:13, Y:5, L:3, Q:10, H:1, I:7, S:5, R:2, E:3, M:1	Total residues of Out	Y:6, V:7, D:16, T:6, A:9, N:17, K:7, F:6, Q:10, H:2, I:6, G:12, S:5, L:2, E:3, R:1
Total residues of mature Omp34	Ala (A): 32 (11.4%), Arg (R): 4 (1.4%), Asn (N): 24 (8.6%), Asp (D): 20 (7.1%) Cys (C): 0 (0.0%), Gln (Q): 15 (5.4%), Glu (E): 9 (3.2%), Gly (G): 30 (10.7%), His (H): 2 (0.7%) Ile (I): 10 (3.6%), Leu (L): 17 (6.1%), Lys (K): 14 (5.0%), Met (M): 4 (1.4%), Phe (F): 15 (5.4%), Pro (P): 8 (2.9%), Ser (S): 13 (4.6%), Thr (T): 20 (7.1%), Trp (W): 1 (0.4%), Tyr (Y): 21 (7.5%), Val (V): 21 (7.5%), Pyl (O): 0 (0.0%), Sec (U): 0 (0.0%)		

structure and the tool could not annotate membrane insertion, which is required for model building.

eThread, FALCON@home, I-TASSER, LOMETS, Phyre2, ROBETTA and RaptorX built 10, 10, 5, 10, 21, 5 and 1models for the query sequence respectively. Amongst models built by Phyre2, only one model covered full-length of the query protein sequence. Two models built by FALCON@home did not cover full-length of the query protein sequence. Table 2 represents the predicted models along with their evaluations. Based on topology analyses, models hit to 14-stranded β-barrels were assumed as more correct ones. Eight models hit to 14-stranded β-barrels among which ROBETTA 5 was the best (based on QMEAN and RAMPAGE analyses) (Table 2).

After model refinement, quality of the model was improved (Table 3 and Fig. 3).

Fig. 4 shows the best refined model of Omp34 kDa.

3.6. Alignments

Sequence alignment length was 320 residues with 11% sequence identity and 48 gaps (Fig. 5).

4. Discussion

Omp33-36 (Omp34 kDa), known as a multifunctional virulence factor, is associated with metabolic fitness of *A. baumannii*, the pathogen adherence and invasion to human epithelial cells (*via* binding to fibronectin) and also its cytotoxicity (Smani et al., 2012). In addition to induce apoptosis and modulate autophagy in human

Table 2
Model evaluations. QMEAN scores and z-scores as well as RAMPAGE results for each model are presented. Phyrestorm hits and their topology are also shown.

Tool/model	QMEAN/z-score	Favored region	Allowed region	Outlier	Phyrestorm	PRED-TMBB	BOCTOPUS
eThread 1	0.148/−6.71	246 (88.5%)	19 (6.8%)	13 (4.7%)	0.96 (2 × E1)	16-stranded	No TM-regions predicted
eThread 2	0.112/−7.09	198 (71.2%)	47 (16.9%)	33 (11.9%)	–	–	–
eThread 3	0.043/−7.84	221 (79.5%)	42 (15.1%)	15 (5.4%)	0.83 (1I78)	16-stranded	–
eThread 4	**0.020/−8.09**	**235 (84.5%)**	**30 (10.8%)**	**13 (4.7%)**	**0.87 (1T16)**	**14-stranded**	**14-stranded**
eThread 5	**0.113/−7.08**	**230 (82.7%)**	**30 (10.8%)**	**18 (6.5%)**	**0.87 (1UYN)**	**14-stranded**	**-**
eThread 6	−0.010/-8.42	194 (69.8%)	55 (19.8%)	29 (10.4%)	–		
eThread 7	0.034/−7.94	241 (86.7%)	25 (9.0%)	12 (4.3%)	0.70 (4RDR)	24-stranded	22-stranded
eThread 8	0.022/−8.07	200 (71.9%)	45 (16.2%)	33 (11.9%)	–		
eThread 9	0.034/−7.94	211 (75.9%)	42 (15.1%)	25 (9.0%)	–		
eThread 10	0.066/−7.6	171 (61.5%)	54 (19.4%)	53 (19.1%)	–		
FALCON@home 1	0.183/−6.33	247 (88.8%)	24 (8.6%)	7 (2.5%)	0.76 (3ROH)	11-stranded	2-stranded
FALCON@home 2	0.292/−5.16	256 (92.1%)	16 (5.8%)	6 (2.2%)	0.67 (2 × 55)	10-stranded	10-stranded
FALCON@home 3	0.284/−5.25	254 (91.4%)	15 (5.4%)	9 (3.2%)	0.84 (3AEH)	12-stranded	12-stranded
FALCON@home 4	0.180/−6.37	235 (84.5%)	30 (10.8%)	13 (4.7%)	0.63 (2Y7L)	13-stranded	–
FALCON@home 5	0.284/−5.24	245 (88.1%)	26 (9.4%)	7 (2.5%)	0.88 (1S1D)	–	–
FALCON@home 7	0.247/−5.64	248 (89.2%)	17 (6.1%)	13 (4.7%)	0.74 (3RG0)	–	–
FALCON@home 9	0.250/−5.61	220 (79.1%)	39 (14.0%)	19 (6.8%)	0.61 (2N18)	–	–
FALCON@home 10	0.283/−5.25	232 (83.5%)	30 (10.8%)	16 (5.8%)	0.66 (2VGD)	9-stranded	2-stranded
I-TASSER 1	**0.240/−5.71**	**157 (56.5%)**	**76 (27.3%)**	**45 (16.2%)**	**0.67 (4V3H)**	**14-stranded**	**-**
I-TASSER 2	0.141/−6.79	178 (64.0%)	55 (19.8%)	45 (16.2%)	0.87 (4RL8)	12-stranded	12-stranded
I-TASSER 3	0.241/−5.71	164 (59.0%)	70 (25.2%)	44 (15.8%)	–		
I-TASSER 4	0.113/−7.09	207 (74.5%)	53 (19.1%)	18 (6.5%)	0.88 (4RL8)	12-stranded	12-stranded
I-TASSER 5	**0.100/−7.23**	**181 (65.1%)**	**60 (21.6%)**	**37 (13.3%)**	**0.66 (2 × 9 K)**	**14-stranded**	**14-stranded**
LOMETS 1	0.084/−7.4	249 (89.6%)	20 (7.2%)	9 (3.2%)	0.61 (2N18)	–	–
LOMETS 2	0.101/−7.22	256 (92.1%)	14 (5.0%)	8 (2.9%)	–	–	–
LOMETS 3	**0.027/−8.02**	**249 (89.6%)**	**22 (7.9%)**	**7 (2.5%)**	**0.76 (1T16)**	**14-stranded**	**14-stranded**
LOMETS 4	0.063/−7.63	259 (93.2%)	12 (4.3%)	7 (2.5%)	–	–	–
LOMETS 5	0.085/−7.39	264 (95.0%)	6 (2.2%)	8 (2.9%)	–	–	–
LOMETS 6	**0.036/−7.92**	**246 (88.5%)**	**22 (7.9%)**	**10 (3.6%)**	**0.63 (3PGU)**	**14-stranded**	**14-stranded**
LOMETS 7	0.132/−6.89	238 (85.6%)	22 (7.9%)	18 (6.5%)	0.85 (1PHO)	16-stranded	16-stranded
LOMETS 8	**0.203/−6.12**	**243 (87.4%)**	**21 (7.6%)**	**14 (5.0%)**	**0.64 (2R4L)**	**14-stranded**	**14-stranded**
LOMETS 9	0.125/−6.96	243 (87.4%)	22 (7.9%)	13 (4.7%)	–		
LOMETS 10	0.148/−6.71	260 (93.5%)	11 (4.0%)	7 (2.5%)	0.65 (4RL8)	12-stranded	12-stranded
Phyre2	0.105/−7.17	210 (75.5%)	38 (13.7%)	30 (10.8%)	–		
ROBETTA 1	0.387/−4.13	244 (87.8%)	26 (9.4%)	8 (2.9%)	0.76 (3O0E)	16-stranded	16-stranded
ROBETTA 2	0.425/−3.72	248 (89.2%)	28 (10.1%)	2 (0.7)	–		
ROBETTA 3	0.311/−4.95	221 (79.5%)	39 (14.0%)	18 (6.5%)	0.78 (4QQ1)	20-stranded	–
ROBETTA 4	0.465/−3.3	219 (78.8%)	45 (16.2%)	14 (5.0%)	0.62 (5AWG)	–	–
ROBETTA 5	**0.416/−3.83**	**243 (87.4%)**	**29 (10.4%)**	**6 (2.2%)**	**0.72 (4D5B)**	**14-stranded**	**-**
RaptorX	0.124/comparison the experimental structures not possible	236 (84.9%)	29 (10.4%)	13 (4.7%)	0.69 (3SY9)		

Toplogically significant.

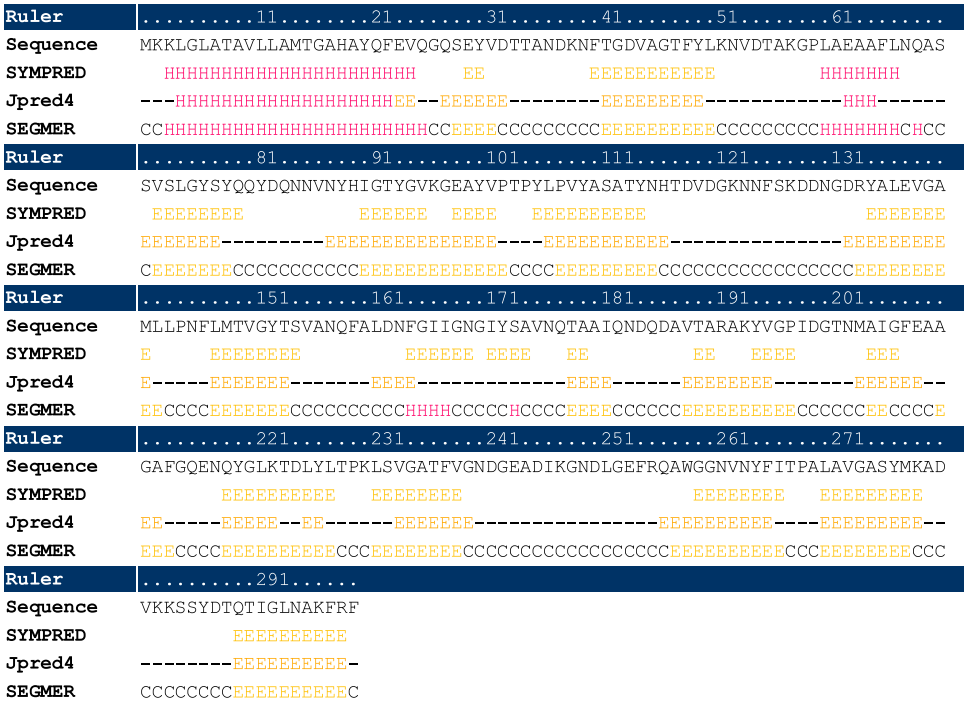

Fig. 2. Predicted secondary structure of Omp33-36 by various tools.
H: helix; E: extended strand; C, dash or blank: Coil

cells, Omp33-36 enables the pathogen to persist inside autophagosomes (Rumbo et al., 2014). Functions of a putative protein are due to its sequence and consequently its structure. Classification of a protein could help in selection of accurate predicted 3D models. Omp33-36 was classified as a β-barrel outer membrane protein. Although identifying β-barrel membrane proteins is challenging since no clear stretches of hydrophobic residues could be detected in their primary sequences (Liang et al., 2012), this prediction is strongly supported by experimental evidence (del Mar Tomás et al., 2005; Rumbo et al., 2014). The method of choice for unveiling high-resolution structures of proteins is X-ray crystallography in which crystallization of a given protein is a critical step (Lacapere et al., 2007). Since Omp33-36 predicted as a low promising crystallization target which could be crystallized very difficult, high failure probability in experimental determination of the protein structure is conceivable. Hence, invoking computational methods with sufficient accuracy to determine the protein structure as an alternative solution is justified (Liang et al., 2012; Marks et al., 2012).

Signal peptide does not exist within the mature protein; so, the detected signal peptide was removed for template selection. Mature protein was consisted of 280 residues. Topology along with secondary structure of a given protein could be recruited to arrive at an accurate 3D model of the protein. Topology of a β-barrel outer membrane protein refers to the number of anti-parallel transmembrane β-strands and the sidedness the *N*- and *C*-terminal ends of the protein (Liang et al., 2012) in which the *N*- and *C*-terminal ends could be usually found on the periplasmic side (Jackups and Liang, 2005). The N and C termini of Omp33-36 are located on the periplasmic side of the β-barrel. For β-barrel membrane proteins, there is an overall "positive-outside" distribution in which their extracellular cap regions are enriched with positively charged Arg and Lys disfavored in the periplasmic cap regions; while, Asp and Glu (acidic residues) could be evenly found in both cap regions (Jackups and Liang, 2005). this could be

Table 3
Refined models and their evaluations.

Refined model	QMEAN/z-score	Favored region	Allowed region	Outlier
ModRefiner	0.296/−5.12	261 (93.9%)	16 (5.8%)	1 (0.4%)
ModRefiner based on 4D5B	0.276/−5.33	265 (95.3%)	12 (4.3%)	1 (0.4%)
3D-refine 1	0.453/−3.42	254 (91.4%)	18 (6.5%)	6 (2.2%)
3D-refine 2	0.460/−3.35	254 (91.4%)	18 (6.5%)	6 (2.2%)
3D-refine 3	0.465/−3.3	255 (91.7%)	17 (6.1%)	6 (2.2%)
3D-refine 4	**0.474/−3.19**	**256 (92.1%)**	**16 (5.8%)**	**6 (2.2%)**
3D-refine 5	0.471/−3.23	255 (91.7%)	17 (6.1%)	6 (2.2%)
GalaxyWEB 1	0.289/−5.19	261 (93.9%)	15 (5.4%)	2 (0.7%)
GalaxyWEB 2	0.367/−4.35	261 (93.9%)	16 (5.8%)	1 (0.4%)
GalaxyWEB 3	0.364/−4.39	261 (93.9%)	16 (5.8%)	1 (0.4%)
GalaxyWEB 4	0.367/−4.35	261 (93.9%)	16 (5.8%)	1 (0.4%)
GalaxyWEB 5	0.322/−4.84	261 (93.9%)	16 (5.8%)	1 (0.4%)
4D5B	0.284	307 (99.0%)	2 (0.6%)	1 (0.3%)

Bold letter indicates the selected model.

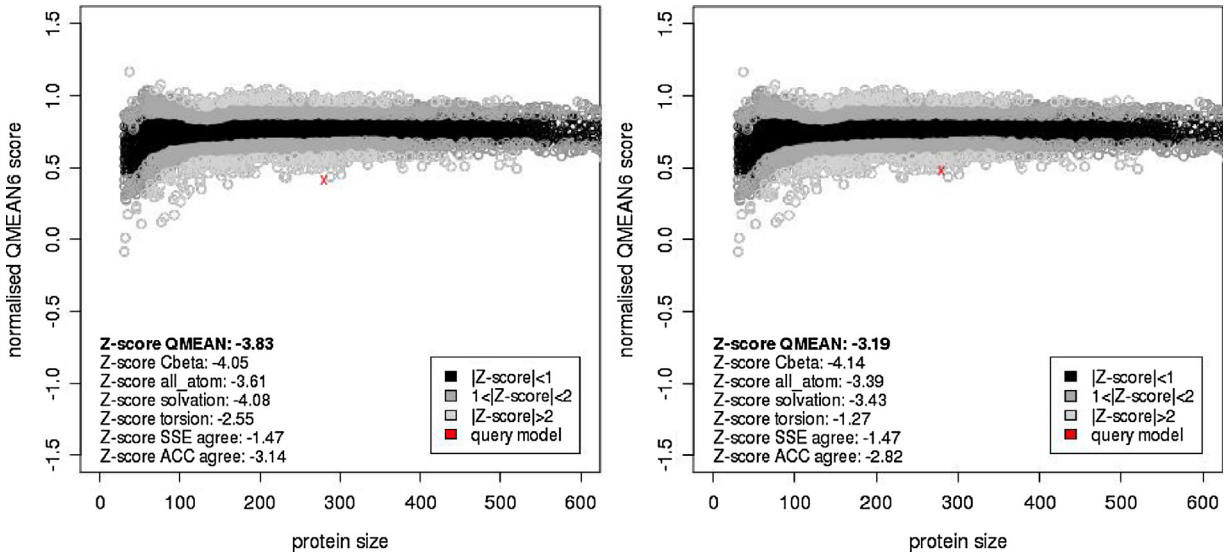

Fig. 3. Estimated absolute model quality plots (QMEAN). Left: primary model; right: the refined model. The colored area represents the QMEAN scores of the reference structures from the PDB. The QMEAN score calculated for the primary and the refined models are compared to those obtain for experimental structures of similar size (model size +/− 10%). The QMEAN Z-score indicates how many standard deviations the predicted QMEAN score differs from expected values for experimental structures.

attributed to the negatively charged lipopolysaccharides (LPS) enriched in the outer-leaflet of the outer membrane (Liang et al., 2012). There are 4 Arg and 14 Lys within the mature Omp33-36 sequence among which about 50% of them are located in extracellular loops. Interestingly, >65% of acidic residues was found in the extracellular loops. Moreover, their periplasmic loops are short compared to their extracellular loops (Schulz, 2000). A discrepancy was seen in position of β2 predicted by BOCTOPUS and PRED-TMBB. To resolve the problem, predicted secondary structure results could be appealed thereby the BOCTOPUS prediction become outstanding. There are 1 Trp and 21 Tyr within the mature Omp33-36 sequence among which >66% of them are located in β-strands. Trp and Tyr are frequently found in transmembrane segments of β-barrel outer membrane proteins (Liang et al., 2012). Pro preferably could be found in the periplasmic cap region (Jackups and Liang, 2005). Mature Omp33-36 has 8 Pro residues among which 7 residues were located in the periplasmic loops.

Selection of an approach to arrive at an accurate 3D model depends on whether appropriate templates sharing high sequence similarity could be found. Homology modeling could be employed as the method of chose with high accuracy when a structure template with sequence identity of >30% is found for a query protein (Floudas et al., 2006). Since the best template obtained from PSI-BLAST shared <10% of sequence similarity with mature Omp33-36 failure of homology modeling was expected.

In such situation, correct prediction from sequence has been hard to achieve (Marks et al., 2012); however, *ab initio* or combination of approaches could serve to resolve this problem. For β-barrel outer membrane proteins, a brilliant strategy is integrating tertiary structure prediction with the topology and secondary structure (Liang et al., 2012; Sefid et al., 2013). Based on

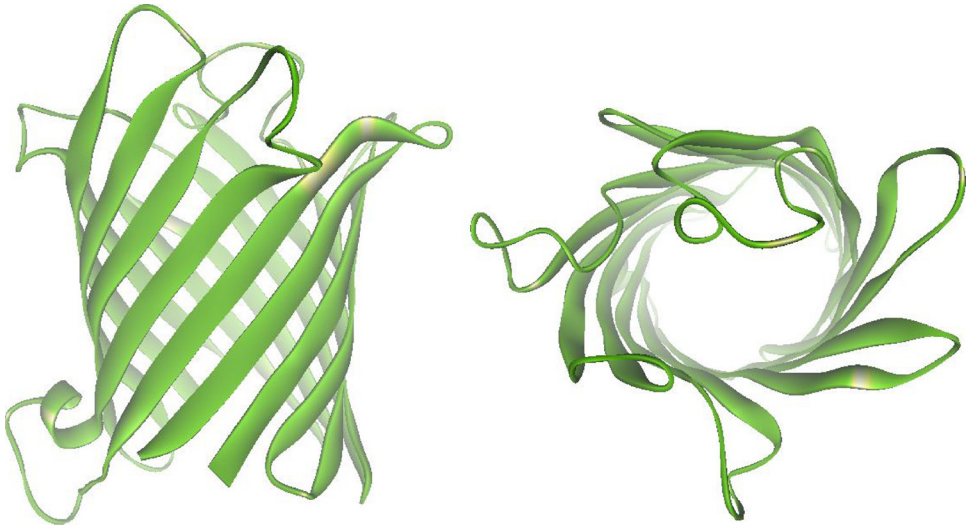

Fig. 4. The best refined structure of Omp33-36. Cartoon models represented from the side (Left) and from the extracellular side (Right).

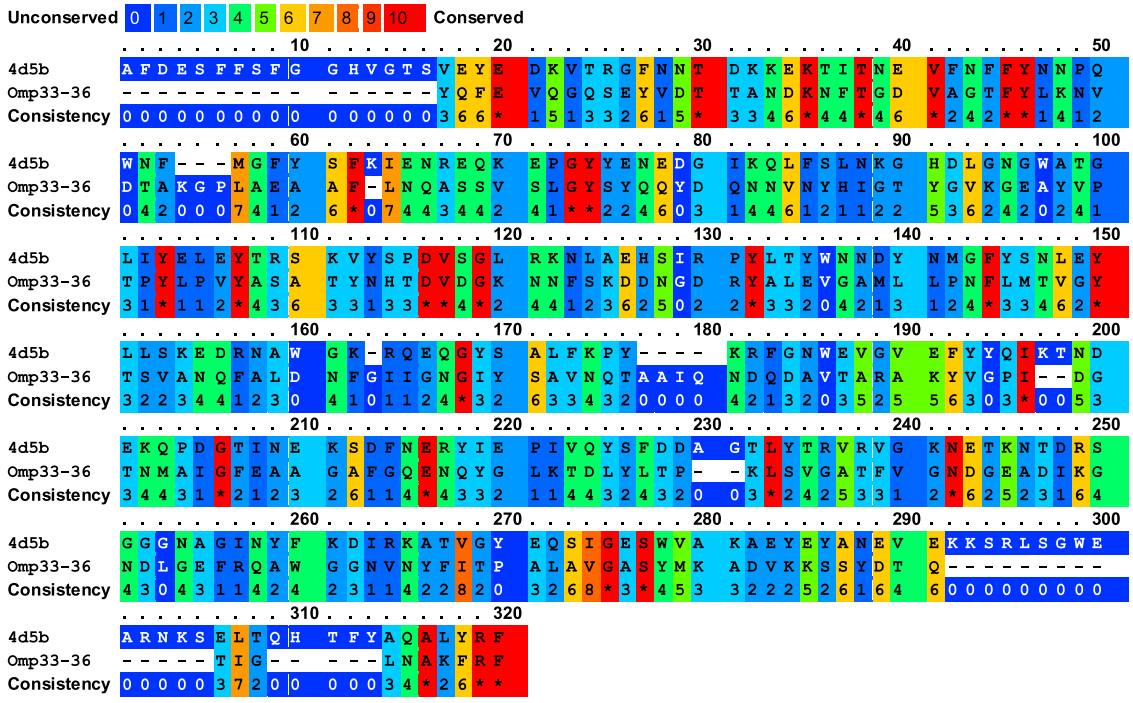

Fig. 5. Sequence alignment of Omp33-36 with CymA.

QMEAN results, all models built by ROBETTA have higher quality than those built by other employed tools. However, incorporation of topology and secondary structure in evaluation, screening and selection processes of the predicted 3D structures could result in arriving at the most reliable model. On one hand, protein structure is more conserved than sequence; hence, identification and then alignment of structurally similar protein(s) to the query could provide biological insights as well as significant clues regarding evolution and functions of the protein (Mezulis et al., 2016). Phyrestorm addressed to this demand thereby, models hitting to 14-stranded β-barrel outer membrane proteins were considered as accurate ones regarding topology. Amongst, the model with the highest quality (QMEAN and RAMPAGE) score was selected as the best. Refinement of a given model is a critical stage in 3D structure prediction process (Petrey and Honig, 2005). After refining the best model, its QMEAN (*z*-) score and Ramachandran plot were improved and fell into QMEAN (*z*-) score area of experimental structures. Sequence alignment of the query protein with the sequence of CymA from *Klebsiella oxytoca* was carried out to pierce into evolutional and functional properties of Omp33-36. As to be expected, there was more structural similarity than sequence similarity. CymA is a ligand-gated OM diffusion channel. It is demonstrated that about 15 resides at the *N*-terminus of CymA forms a mobile element able to move in and out of the barrel, thereby the permeability of the outer membrane could be preserved (van den Berg et al., 2015). This region does not exist in Omp33-36 structure which is in concordance with its porin functions previously reported (del Mar Tomás et al., 2005). A truncated CymA in which the first 15 residues were removed was converted to a completely open channel (van den Berg et al., 2015). In addition to Omp33-36 porin function, carbapenem-resistance associated with the loss of this protein could also be justified by this model.

In conclusion, the achieved 3D structure concurring with topology and function of the protein as well as previous experimental evidence could be considered as an accurate reliable model paving the road toward drug and vaccine design against *A. baumannii*.

Conflict of interest

The authors declare that they have no conflict of interest.

Acknowledgments

The authors wish to thank Shahed University for supporting the conduct of this research. The authors appreciate National Institute for Medical Research Development grant number 942282.

References

Bagos, P.G., Liakopoulos, T.D., Hamodrakas, S.J., 2004a. Finding beta-barrel outer membrane proteins with a Markov chain model. WSEAS Trans. Biol. Biomed. 2, 186–189.

Bagos, P.G., Liakopoulos, T.D., Spyropoulos, I.C., Hamodrakas, S.J., 2004b. PRED-TMBB: a web server for predicting the topology of β-barrel outer membrane proteins. Nucleic Acids Res. 32, W400–W404.

Benkert, P., Künzli, M., Schwede, T., 2009. QMEAN server for protein model quality estimation. Nucleic Acids Res. 37, W510–W514.

Berven, F.S., Flikka, K., Jensen, H.B., Eidhammer, I., 2004. BOMP: a program to predict integral β-barrel outer membrane proteins encoded within genomes of gram-negative bacteria. Nucleic Acids Res. 32, W394–W399.

Bhattacharya, D., Nowotny, J., Cao, R., Cheng, J., 2016. 3Drefine: an interactive web server for efficient protein structure refinement. Nucleic Acids Res. gkw336.

Brylinski, M., Lingam, D., 2012. e Thread: a highly optimized machine learning-based approach to meta-threading and the modeling of protein tertiary structures. PLoS One 7, e50200.

Dijkshoorn, L., Nemec, A., Seifert, H., 2007. An increasing threat in hospitals: multidrug-resistant *Acinetobacter baumannii*. Nat. Rev. Microbiol. 5, 939–951.

Drozdetskiy, A., Cole, C., Procter, J., Barton, G.J., 2015. JPred4: a protein secondary structure prediction server. Nucleic Acids Res. 43, W389–W394.

Ebejer, J.-P., Hill, J.R., Kelm, S., Shi, J., Deane, C.M., 2013. Memoir: template-based structure prediction for membrane proteins. Nucleic Acids Res. 41, W379–W383.

Fajardo Bonin, R., Chapeaurouge, A., Perales, J., da Silva Jr, J.G., do Nascimento, H.J., D'Alincourt Carvalho Assef, A.P., Senna, M., Procópio, J., 2014. Identification of immunogenic proteins of the bacterium *Acinetobacter baumannii* using a proteomic approach. PROTEOM-Clin. Appl. 8, 916–923.

Floudas, C., Fung, H., McAllister, S., Mönnigmann, M., Rajgaria, R., 2006. Advances in protein structure prediction and de novo protein design: a review. Chem. Eng. Sci. 61, 966–988.
Gaete-Eastman, C., Morales-Quintana, L., Herrera, R., Moya-León, M.A., 2015. In-silico analysis of the structure and binding site features of an α-expansin protein from mountain papaya fruit (VpEXPA2), through molecular modeling, docking, and dynamics simulation studies. J. Mol. Model. 21, 1–12.
Haste Andersen, P., Nielsen, M., Lund, O., 2006. Prediction of residues in discontinuous B-cell epitopes using protein 3D structures. Protein Sci. 15, 2558–2567.
Hayat, S., Elofsson, A., 2012. BOCTOPUS: improved topology prediction of transmembrane β barrel proteins. Bioinformatics 28, 516–522.
Heo, L., Park, H., Seok, C., 2013. GalaxyRefine: protein structure refinement driven by side-chain repacking. Nucleic Acids Res. 41, W384–W388.
Islam, A.H., Singh, K.K., Ismail, A., 2011. Demonstration of an outer membrane protein that is antigenically specific for *Acinetobacter baumannii*. Diagn. Microbiol. Infect. Dis. 69, 38–44.
Jackups, R., Liang, J., 2005. Interstrand pairing patterns in β-barrel membrane proteins: the positive-outside rule, aromatic rescue, and strand registration prediction. J. Mol. Biol. 354, 979–993.
Jahandideh, S., Jaroszewski, L., Godzik, A., 2014. Improving the chances of successful protein structure determination with a random forest classifier. Acta Crystallogr. Sect. D: Biol. Crystallogr. 70, 627–635.
Jahangiri, A., Rasooli, I., Owlia, P., Fooladi, A.A.I., Salimian, J., 2017. In silico design of an immunogen against *Acinetobacter baumannii* based on a novel model for native structure of outer membrane protein A. Microb. Pathog. 105, 201–210.
Juncker, A.S., Willenbrock, H., Von Heijne, G., Brunak, S., Nielsen, H., Krogh, A., 2003. Prediction of lipoprotein signal peptides in gram-negative bacteria. Protein Sci. 12, 1652–1662.
Källberg, M., Wang, H., Wang, S., Peng, J., Wang, Z., Lu, H., Xu, J., 2012. Template-based protein structure modeling using the RaptorX web server. Nat. Protoc. 7, 1511–1522.
Kelley, L.A., Mezulis, S., Yates, C.M., Wass, M.N., Sternberg, M.J., 2015. The Phyre2 web portal for protein modeling, prediction and analysis. Nat. Protoc. 10, 845–858.
Khalili, S., Jahangiri, A., Borna, H., Ahmadi Zanoos, K., Amani, J., 2014. Computational vaccinology and epitope vaccine design by immunoinformatics. Acta Microbiol. Immunol. Hung. 61, 285–307.
Khalili, S., Mohammadpour, H., Shokrollahi, M., 2016. ILP −2 Modeling and Virtual Screening of a FDA Approved Library: A Possible Anticancer Therapy. .
Khalili, S., Rasaee, M., Bamdad, T., 2017a. 3D structure of DKK1 indicates its involvement in both canonical and non-canonical Wnt pathways. Mol. Biol. 51, 155–166.
Khalili, S., Jahangiri, A., Hashemi, Z.S., Khalesi, B., Mardsoltani, M., Amani, J., 2017b. Structural pierce into molecular mechanism underlying *Clostridium perfringens* epsilon toxin function. Toxicon 127, 90–99.
Kim, D.E., Chivian, D., Baker, D., 2004. Protein structure prediction and analysis using the Robetta server. Nucleic Acids Res. 32, W526–W531.
Lacapere, J.-J., Pebay-Peyroula, E., Neumann, J.-M., Etchebest, C., 2007. Determining membrane protein structures: still a challenge!. Trends Biochem. Sci. 32, 259–270.
Liang, J., Naveed, H., Jimenez-Morales, D., Adamian, L., Lin, M., 2012. Computational studies of membrane proteins: models and predictions for biological understanding. Biochim. Biophys. Acta (BBA)-Biomembr. 1818, 927–941.
Malathi, K., Anbarasu, A., Ramaiah, S., 2017. Exploring the resistance mechanism of imipenem in carbapenem hydrolysing class D beta-lactamases OXA-143 and its variant OXA-231 (D224A) expressing Acinetobacter baumannii: an in-silico approach. Comput. Biol. Chem. 67, 1–8.
Marks, D.S., Hopf, T.A., Sander, C., 2012. Protein structure prediction from sequence variation. Nat. Biotechnol. 30, 1072–1080.
Martí, S., Sanchez-Cespedes, J., Oliveira, E., Bellido, D., Giralt, E., Vila, J., 2006. Proteomic analysis of a fraction enriched in cell envelope proteins of Acinetobacter baumannii. Proteomics 6, S82–S87.
McConnell, M.J., Rumbo, C., Bou, G., Pachón, J., 2011. Outer membrane vesicles as an acellular vaccine against *Acinetobacter baumannii*. Vaccine 29, 5705–5710.
McConnell, M.J., Actis, L., Pachón, J., 2013. *Acinetobacter baumannii*: human infections, factors contributing to pathogenesis and animal models. FEMS Microbiol. Rev. 37, 130–155.
Mezulis, S., Sternberg, M.J.E., Kelley, L.A., 2016. PhyreStorm: a web server for fast structural searches against the PDB. J. Mol. Biol. 428, 702–708.
Mihăşan, M., 2010. Basic protein structure prediction for the biologist: a review. Arch. Biol. Sci. 62, 857–871.
Mohammadpour, H., Khalili, S., Hashemi, Z.S., 2015. Kremen is beyond a subsidiary co-receptor of Wnt signaling: an in silico validation. Turk. J. Biol. 39, 501–510.
Mohammadpour, H., Pourfathollah, A.A., Zarif, M.N., Khalili, S., 2016. Key role of Dkk3 protein in inhibition of cancer cell proliferation: an in silico identification. J. Theor. Biol. 393, 98–104.
Nezafat, N., Karimi, Z., Eslami, M., Mohkam, M., Zandian, S., Ghasemi, Y., 2016. Designing an efficient multi-epitope peptide vaccine against Vibrio cholerae via combined immunoinformatics and protein interaction based approaches. Comput. Biol. Chem. 62, 82–95.
Ou, Y.-Y., Gromiha, M.M., Chen, S.-A., Suwa, M., 2008. TMBETADISC-RBF: discrimination of-barrel membrane proteins using RBF networks and PSSM profiles. Comput. Biol. Chem. 32, 227–231.
Ou, Y.Y., Chen, S.A., Gromiha, M.M., 2010. Classification of transporters using efficient radial basis function networks with position-specific scoring matrices and biochemical properties. Proteins: Struct. Funct. Bioinfor. 78, 1789–1797.
Ou, Y.Y., Chen, S.A., Chang, Y.M., Velmurugan, D., Fukui, K., Michael Gromiha, M., 2013. Identification of efflux proteins using efficient radial basis function networks with position-specific scoring matrices and biochemical properties. Proteins: Struct. Funct. Bioinfor. 81, 1634.
Petrey, D., Honig, B., 2005. Protein structure prediction: inroads to biology. Mol. Cell 20, 811–819.
Pirovano, W., Feenstra, K.A., Heringa, J., 2008. PRALINE™: a strategy for improved multiple alignment of transmembrane proteins. Bioinformatics 24, 492–497.
Remmert, M., Linke, D., Lupas, A.N., Söding, J., 2009. HHomp—prediction and classification of outer membrane proteins. Nucleic Acids Res. gkp325.
Rumbo, C., Tomás, M., Moreira, E.F., Soares, N.C., Carvajal, M., Santillana, E., Beceiro, A., Romero, A., Bou, G., 2014. The Acinetobacter baumannii Omp33-36 porin is a virulence factor that induces apoptosis and modulates autophagy in human cells. Infect. Immun. 82, 4666–4680.
Schulz, G.E., 2000. β-barrel membrane proteins. Curr. Opin. Struct. Biol. 10, 443–447.
Sefid, F., Rasooli, I., Jahangiri, A., 2013. In silico determination and validation of baumannii acinetobactin utilization a structure and ligand binding site. BioMed Res. Int. 2013.
Sefid, F., Rasooli, I., Jahangiri, A., Bazmara, H., 2015. Functional exposed amino acids of BauA as potential immunogen against *Acinetobacter baumannii*. Acta Biotheor. 63, 129–149.
Simossis, V., Heringa, J., 2004. Optimally Segmented Consensus Secondary Structure Prediction. Bioinformatics.
Slabinski, L., Jaroszewski, L., Rychlewski, L., Wilson, I.A., Lesley, S.A., Godzik, A., 2007. XtalPred: a web server for prediction of protein crystallizability. Bioinformatics 23, 3403–3405.
Smani, Y., McConnell, M.J., Pachón, J., 2012. Role of fibronectin in the adhesion of *Acinetobacter baumannii* to host cells. PLoS One 7, e33073.
Smani, Y., Dominguez-Herrera, J., Pachón, J., 2013. Association of the outer membrane protein Omp33 with fitness and virulence of *Acinetobacter baumannii*. J. Infect. Dis. 208, 1561–1570.
Vila, J., Pachón, J., 2012. Therapeutic options for *Acinetobacter baumannii* infections: an update. Expert Opin. Pharmacother. 13, 2319–2336.
Wang, S., Sheng, W., Chang, Y., Wang, L., Lin, H., Chen, M., Pan, H., Ko, W., Chang, S., Lin, F., 2003. Healthcare-associated outbreak due to pan-drug resistant *Acinetobacter baumannii* in a surgical intensive care unit. J. Hosp. Infect. 53, 97–102.
Wang, C., Zhang, H., Zheng, W.-M., Xu, D., Zhu, J., Wang, B., Ning, K., Sun, S., Li, S.C., Bu, D., 2015. FALCON@ home: a high-throughput protein structure prediction server based on remote homologue recognition. Bioinformatics btv581.
Wu, S., Zhang, Y., 2007. LOMETS: a local meta-threading-server for protein structure prediction. Nucleic Acids Res. 35, 3375–3382.
Wu, S., Zhang, Y., 2010. Recognizing protein substructure similarity using segmental threading. Structure 18, 858–867.
Xu, D., Zhang, Y., 2011. Improving the physical realism and structural accuracy of protein models by a two-step atomic-level energy minimization. Biophys. J. 101, 2525–2534.
Yang, J., Yan, R., Roy, A., Xu, D., Poisson, J., Zhang, Y., 2015. The I-TASSER suite: protein structure and function prediction. Nat. Methods 12, 7–8.
del Mar Tomás, M., Beceiro, A., Pérez, A., Velasco, D., Moure, R., Villanueva, R., Martínez-Beltrán, J., Bou, G., 2005. Cloning and functional analysis of the gene encoding the 33-to 36-kilodalton outer membrane protein associated with carbapenem resistance in *Acinetobacter baumannii*. Antimicrob. Agents Chemother. 49, 5172–5175.
van den Berg, B., Bhamidimarri, S.P., Prajapati, J.D., Kleinekathöfer, U., Winterhalter, M., 2015. Outer-membrane translocation of bulky small molecules by passive diffusion. Proc. Natl. Acad. Sci. U. S. A. 112, E2991–E2999.